Eur Biophys J (2007) 36:1071–1082
DOI 10.1007/s00249-007-0195-6

ORIGINAL PAPER

Molecular dynamics simulation approach for the prediction of transmembrane helix–helix heterodimers assembly

Oumarou Samna Soumana · Norbert Garnier · Monique Genest

Received: 16 February 2007 / Revised: 11 May 2007 / Accepted: 15 May 2007 / Published online: 24 July 2007

Abstract Computational methods are useful to identify favorable structures of transmembrane (TM) helix oligomers when experimental data are not available or when they cannot help to interpret helix–helix association. We report here a global search method using molecular dynamics (MD) simulations to predict the structures of transmembrane homo and heterodimers. The present approach is based only on sequence information without any experimental data and is first applied to glycophorin A to validate the protocol and to the HER2-HER3 heterodimer receptor. The method successfully reproduces the experimental structures of the TM domain of glycophorin A (GpA_{TM}) with a root mean square deviation of 1.5 Å. The search protocol identifies three energetically stable models of the TM domain of HER2-HER3 receptor with favorable helix–helix arrangement, including right-handed and left-handed coiled-coils. The predicted TM structures exhibit the GxxxG-like motif at the dimer interface which is presumed to drive receptor oligomerization. We demonstrate that native structures of TM domain can be predicted without quantitative experimental data. This search protocol could help to predict structures of the TM domain of HER heterodimer family.

Presented at the joint biannual meeting of the SFB-GEIMM-GRIP, Anglet France, 14–19 October 2006.

O. Samna Soumana (✉) · N. Garnier · M. Genest
Centre de Biophysique Moléculaire, UPR 4301, CNRS,
University of Orléans, rue Charles Sadron,
45071 Orléans Cedex 02, France
e-mail: soumana@cnrs-orleans.fr

O. Samna Soumana
INSERM, rue Charles Sadron,
45071 Orléans Cedex 02, France

Keywords Molecular dynamics global search · Helix–helix association · Glycophorin A · ErbB/HER receptor

Introduction

Membrane proteins encoded by nearly ~20–30% of the genome (Krogh et al. 2001; White 2004) are involved in complex signaling and transport functions. Because of their crucial role in many cellular processes they constitute the most biologically important family of proteins that serve as targets for drug discovery. However, their great biological importance contrasts with the very small number of structures resolved at high-resolution (Jayasinghe et al. 2001; White et al. 2001; Berman et al. 2002; White 2004). Solving membrane protein structures is necessary for a complete understanding of cellular processes (Fleishman and Ben-Tal 2006a, b). To overcome the difficulties to express membrane proteins and to obtain experimental structure using X-ray crystallography (White 2004) and nuclear magnetic resonance (NMR) (Opella and Marassi 2004) various computational methods for predicting the topology and the packing of transmembrane (TM) helices have been developed. Helical proteins are the dominant class of TM proteins and the identification of sequence segments embedded in membranes represents the fundamental step to progress into the membrane protein folding problem (Krogh et al. 2001; Chen et al. 2002; Kim et al. 2003; Kokubo and Okamoto 2004; Akula and Pattabiraman 2005; Adamian and Liang 2006; Fleishman et al. 2006b). Another step is to predict how TM helices associate. Various computational approaches have been developed all based on the two-stage model of membrane protein folding (Popot and Engelman 1990). The two simple rules are that helices are individually

inserted into the plasma membrane, and next, helices associate to shape the tertiary structure of the protein.

Specific interactions take place between hydrophobic segments within the bilayer and the major contribution to helix–helix interactions in membrane comes from van der Waals packing (Popot and Engelman 1990; White and Wimley 1999). Therefore, modeling approaches including molecular dynamics (MD) simulations and energy minimizations, combined with experimental information clearly identify structures of helix bundles (Herzyk and Hubbard 1995; Fleishman et al. 2004; Beuming and Weinstein 2005; Fleishman and Ben-Tal 2006a, b).

Computational methods can be used also to identify the most favorable interactions between TM helices when biochemical and biophysical data have no existence or when they cannot help to interpret helix–helix association. The best example is that of the TM dimer of glycophorin A (GpA) for which global search MD studies (Treutlein et al. 1992; Adams et al. 1995, 1996) had first identified the structural model of the dimer, latter solved by NMR experiments in micelles (MacKenzie et al. 1997). Exhaustive studies have been undertaken to explore the determinants of stability in GpA dimerization highlighting the role of small residue sequences called the GxxxG motif, in mediating inter helix contacts (Russ and Engelman 2000). GxxxG-like motifs in which Gly residue is substituted by a small residue like Ala, Ser and Thr are frequently found in mediating TM helix association in a variety of protein families, like signal transduction proteins, channels, transporters and enzymes (Eilers et al. 2000; Dawson et al. 2002; Senes et al. 2004).

This motif is present in the TM domains of all the members of the HER family of growth factor receptor tyrosine kinase (ErbB1/HER or EGFR; ErbB2/HER2, ErbB3/HER3, ErbB4/HER4). Activation of HER receptors involves ligand-induced oligomerization, which in turn leads to receptor trans-phosphorylation and activation within dimers or higher order oligomers (Schlessinger 2000). Subsequent studies have shown that interactions between TM domains do contribute significantly to homo and hetero dimerization processes (Tanner and Kyte 1999; Mendrola et al. 2002). The single TM domain of HER members exhibits a conserved GxxxG-like motif at the N-terminal and the C-terminal ends. The $HER^{3}{}_{TM}$ domain exhibits this motif only at the N-terminus. Mutational analyses suggest that TM dimerization may involve one of the two motifs for a separate function (Fleishman et al. 2002; Mendrola et al. 2002). As an example, in the case of the $HER^{1}{}_{TM}$ and $HER^{2}{}_{TM}$ one motif at the C-terminus serves for homo dimerization and the other at the N-terminus for heterodimerization (Gerber et al. 2004).

Multiple short MD simulations in vacuum have been used to identify possible structures of the TM domain association of the HER2/Neu receptors demonstrating the importance of the GxxxG-like motif in the formation of homodimers in the wild and the oncogenic forms (Garnier et al. 1997; Duneau et al. 1999a, b; Sajot and Genest 2000).

Besides the fact that the dimerization motif is involved in the association of the TM domain of the HER receptors, structural data on TM heterodimers are still unknown.

In this paper we describe a computational method that allows the prediction of structural models of HER heterodimers. For that, we have revisited our MD search protocol used to model helix–helix packing of symmetric homodimers (Garnier et al. 1997; Duneau et al. 1999a, b). In the case of heterodimers, symmetry constraints cannot be used and the overall energy surface has to be explored. The conformational sampling is described by the rotational pitch angle of each helix allowing the complete exploration of helix–helix interfaces.

Structural data of heterodimers of TM helices are not yet available (Caballero-Herrera and Nilsson 2003) and to test our search method it is first applied to the GpA_{TM} dimer and second to the HER2-HER3 TM domain. HER2 is the preferred dimerization partner of all HER receptors and preferentially associate to HER3 (Tzahar et al. 1996; Graus-Porta et al. 1997). HER2-HER3 heterodimer shows the strongest potency in terms of stimulating cell proliferation (Pinkas-Kramarski et al. 1996; Rubin and Yarden 2001; Citri et al. 2003).

Our method successfully describes the right-handed structure of the GpA_{TM} dimer with a root mean square deviation (RMSD) of 1.5 Å from the experimental structure (MacKenzie et al. 1997).

The excellent agreement obtained for GpA_{TM} dimer leads us to explore TM domain structures of HER^{2-3}. Experimental information relies on the presence of the GxxxG-like motif at the dimer interface. Our prediction shows that three MD models, with helices in right-handed and left-handed interactions conform to the presence of the GxxxG-like motif in the dimer interface.

Methods

TM domain systems

Two helical dimers are studied. The first one is the dimer of the GpA_{TM} domain (MacKenzie et al. 1997) which is used as template to validate the method. Both helices comprise 23 residues from residue Ile73 to Ile95 constituting the hydrophobic sequence of the TM domain (Tomita et al. 1978). The second one results from the association of the HER2 and HER3 receptors referred to as the $HER^{2-3}{}_{TM}$ domain in the following. Each helix comprises the 25 residues of the hydrophobic sequence of the TM domains of

Table 1 Sequence of the TM domains

Protein	Sequence	Residues
GpA_{TM}	ITLIIFGVMAGVIGTILLISYGI	73- 95
$HER2_{TM}$	LTSIVSAVVGILLVVVLGVVFGILI	651-675
$HER3_{TM}$	LTMALTVIAGLVVIFMMLGGTFLYW	642-666

The sequences of $HER^2{}_{TM}$ (Coussens et al. 1985; Yamamoto et al. 1986; Ehsani et al. 1993) and $HER^3{}_{TM}$ (Kraus et al. 1989) are listed, alongside the GpA_{TM} sequence. Regions corresponding to the potential GxxxG dimerization motifs in each TM domain are shaded gray

the receptors (Coussens et al. 1985; Yamamoto et al. 1986; Kraus et al. 1989; Ehsani et al. 1993). The sequences of the two systems are given in Table 1. For both systems, each helix has the amino terminus acetylated and the carboxyl terminus methyl-aminated to mimic the peptide bond.

Global search method

All calculations were undertaken by using the program CHARMM Version 26 (Brooks et al. 1983) and the all hydrogen PARAM22 force field (MacKerell et al. 1992). All calculations were carried out in vacuum and the dielectric constant was set to 1.0. This value is a good approximation of the membrane environment (Adams et al. 1995; Duneau et al. 1999a, b) and is justified for our purpose to define a set of possible structures of the TM dimers. Electrostatic interactions were not truncated and an atom-based switching function was used for the van der Waals interactions between 10 and 12 Å. The nonbonded list was generated with a cutoff of 13 Å. All calculations were performed on a multi-processor platform Linux Beowulf clusters with dual 3.06 GHz Intel Xeon processors.

Conformational sampling

A parallel dimer was first generated with the two helices (H1 and H2) built with the standard torsion angles ($\varphi = -57°$, $\psi = -47°$) and the helix axes aligned along the *Z*-axis. This initial construction corresponding to two superimposed helices was used to generate multiple configurations of the dimer by rotating each helix about its own axis. θ_1 and θ_2 are the rotational angles of H1 and H2, respectively. For a complete search over the two-body rotational interaction space, θ_1 was increased by 10° steps from 0° to 360° and, for each θ_1 value, θ_2 was varied by 10° steps from 0° to 360°. A total of 1,296 (36 × 36) initial configurations was generated.

For each of these configurations, helix H2 was translated along the *X*-axis from its initial position (0 Å) by a distance *D* of 20 Å between the two helix axes sufficiently large to avoid atomic contacts. *D* was gradually decreased by increment of 0.25 Å to reach the distance Dh for which the two helices are in favorable interactions. Dh is obtained as follows: at each translation step, the system was energy minimized using first the steepest descent (SD) method and then the Adopted Basis Newton–Raphston (ABNR) minimization algorithm for 50–100 steps. During the minimization process the two helices have been maintained in a parallel orientation by fixing the backbone atoms for the optimization of the side chain orientation. For the 1,296 minimized structures Dh ranges from 9.0 to 11 Å. These minimized structures have been used as starting structures for the simulations. This minimization process has been applied to the GpA_{TM} dimer and to the $HER^{2-3}{}_{TM}$ dimer.

Molecular dynamics protocol

Molecular dynamics simulations were carried out at constant temperature $T = 300$ K. The SHAKE algorithm (Ryckaert et al. 1977) was applied to fix all the bonds involving hydrogen atoms. The integration time step was 1 fs. The MD protocol begins by a heating period (18 ps) during which the system was gradually thermalized from 0 to 300 K by increment of 50 K. New atomic random velocities were assigned from a Maxwell distribution at each temperature step. The α helical structure was maintained by restraining the O_i–NH_{i+4} distance of the backbone hydrogen bonds (Hbonds) at 2.8 Å. The vertical shift of one helix relatively to the second helix along the *Z*-axis was

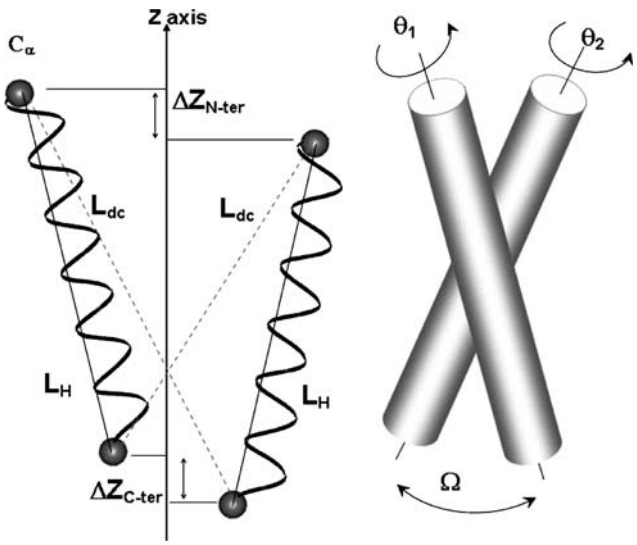

Fig. 1 Parameters defining structure quality, L_H: distance between the C_α atoms of the first residue $C_\alpha{}^H$Nter and the last residue $C_\alpha{}^H$Cter; L_{dc}:crossed distance $C_\alpha{}^{H1}$Nter–$C_\alpha{}^{H2}$Cter and $C_\alpha{}^{H2}$Nter–$C_\alpha{}^{H1}$Cter; Δdc: difference between the crossed distances. $\Delta Z(\text{Nter}) = |\ (Z(C_\alpha{}^{H1}\text{Nter}) - Z(C_\alpha{}^{H2}\text{Nter})\ |$: difference in *Z* positions of the C_α atoms of the first residue of H1 and H2; $\Delta Z(\text{Cter}) = |\ (Z(C_\alpha{}^{H1}\text{Cter}) - Z(C_\alpha{}^{H2}\text{Cter})\ |$: difference in the *Z* positions of the C_α atoms of the last residue of H1 and H2. Ω (°): crossing angle. θ_1 and θ_2 are the rotational angles of H1 and H2, respectively, about their own axis

monitored by applying harmonic crossed distance restraints L_{dc} (see Fig. 1 for definition) at 35 Å and 36 Å with a force constant of 250 kcal mol^{-1} Å^{-2} for the GpA_{TM} dimer and the $HER^{2-3}{}_{TM}$ dimer, respectively. The values are based on those measured on the experimental model of the GpA_{TM} dimer (MacKenzie et al. 1997) and our previous MD models of $HER^{2}{}_{TM}$ homodimers (Sajot and Genest 2000).

Equilibration was continued for 1 ns applying the same α Hbonds and crossed distances restraints with a force constant of 250 kcal mol^{-1} Å^{-2} for the first 300 ps and reduced to 150 kcal mol^{-1} Å^{-2} for the following 300 ps. The last 400 ps were continued without any constraint allowing the two helices to move freely. During the heating and the equilibration periods helix–helix separation D was not restrained.

The production period was conducted during 3 ns without any restraint. Atomic coordinates and energy terms were saved every ps. The last ns was used for averaging and further analysis.

Analysis of helix–helix assembly

Geometric criteria

Several geometrical parameters were used to evaluate the quality of the simulated structures. These parameters, shown in Fig. 1, are: (1) the helix length L_H defined as the distance between the C_α atoms of the first residue at the N-terminus ($C_\alpha{}^{H}$Nter) and of the last residue at the C-terminus ($C_\alpha{}^{H}$Cter). The L_H value informs directly on helix elongation or helix contraction resulting from 3_{10} or π helix distortions. Distortions of the helical backbone are currently observed during MD simulations. We have considered, after several tests that a α helix is structurally correct when L_H does not deviate up to 3 Å from 32 Å for the GpA helix and 35 Å for the HER helix. For a canonical α helix, L_H is about 35.25 Å for a 25 residues helix (HER_{TM}) and 32.5 Å for a 23 residues helix (GpA_{TM}). These values are close to those measured along the Z-axis. One may notice that L_H can also be obtained from the calculation of the helix length along the Z-axis. However, the helix axis is not correctly defined in this case because the α helix structure is not strictly maintained after MD simulations. (2) The difference between the two crossed distances (L_{dc}). This parameter noted Δ_{dc} allows the control of both the vertical shift of the helices and the length of the two helices. (3) The helix register ΔZ defines the vertical position of the helices relatively to each other. It is calculated as the difference between the Z positions of the C_α atoms of the first and the last residues of H1 and H2 along the dimer axis. For bitopic membrane proteins a significant shift of the TM helices along the membrane normal would be impossible due to the limitations imposed by the lipid bilayer (Killian and von Heijne 2000; Killian 2003). (4) The crossing angle Ω, which measures the angle between the two helical axes whereby positive and negative values indicate a left-handed and a right-handed coiled-coil. A distribution of the crossing angle values ranging from –65° to 45° is in accordance with the various studies on membrane protein assembly (Bowie 1997; Chothia et al. 1981; Bywater et al. 2001; Kallblad and Dean 2004). Bowie (1997) examined a small database of helical membrane proteins and showed that a crossing angle of +20° was the most common, in contrast to the globular proteins where packing angles around –35° are the most prevalent. According to Chothia et al. (1981) inter-helical crossing angles range between –80° and +40°. Values of the geometric parameters used to define the dimer structures quality are given in Table 2.

Structure selection

Geometry-based filters

The quality of a dimer structure was determined from the analysis of the 250 configurations extracted from the last ns MD trajectory (one configuration extracted every 4 ps). The structure selection follows several steps:

(1) For each of the 250 configurations, the 6 parameters defined previously were calculated. A score value of 1 is given when one parameter is respected otherwise the score value is 0. A configuration is assumed structurally correct for a total score of 6 or close to correct for a total score of 5. Otherwise, the configuration is rejected. (2) A structure is retained if 80% of the analyzed configurations (N) are structurally correct ($N \geq 200$). Otherwise, the structure is rejected. Steps (1) and (2) applied to the 1,296 structures drastically reduce the number of structurally correct dimers. (3) Based on the distribution of the crossing angle, the remaining structures are clustered into three distinct families of coiled-coils corresponding to right-handed dimers ($\Omega < -10°$), parallel dimers ($-10° \leq \Omega \leq 10°$) and left-handed dimers ($\Omega > 10°$). (4) For each family, several clusters including structures with a Cα RMSD value ≤ 2 Å are well identified. The average structure for each cluster was then energy minimized in order to remove bad contacts

Table 2 Parameters defining dimer structure quality

	L_H (Å)		Δdc (Å)	ΔZ_{Nter} ΔZ_{Cter} (Å)	Ω (°)	
	Min	Max			Min	Max
$HER^{2-3}{}_{TM}$	32.0	38.0	≤3.5	≤3.5	–65°	+45°
GpA_{TM}	29.0	35.0	≤3.5	≤3.5	–65°	+45°

Minimum and maximum values of L_H are defined from the length of a α canonical helix ($L_{H\alpha}$ = 35.25 Å for the HER_{TM} helix and 32.5 Å for the GpA_{TM} helix). Ω (°) is the crossing angle. Minimum and maximum values derived from Bowie (1997) and statistical analysis of membrane proteins. All these parameters are shown in Fig. 1

and was used as the starting point for further MD refinement. The same exact MD protocol described previously was applied.

In addition, it has been applied to the two experimental models of the GpA_{TM} dimer, (model 16 and the average NMR structure) for comparison (see section "Results and discussion").

Interface surface area calculation

The interface surface area (SA) was calculated as the difference between the solvent accessible SA of individual helices and the solvent accessible SA calculated for the dimer. Surface areas are calculated with CHARMM and values are averaged over the last ns of the simulation.

Residues in the TM helices were divided in three groups: interacting residues have over 80% of their SA buried in the helical dimer, partially buried residues have buried SAs between 50 and 80% and exposed residues have more than 50% of their SA accessible (Gimpelev et al. 2004).

Binding free energy calculation

We have calculated the gas-phase contribution to the binding free energy, $\Delta G°_{bind}$ defined as: (Zoete et al. 2005)

$$\text{Vacuo}\ (\text{Helix1} + \text{Helix2} \overset{\Delta G°_{bind}}{\rightarrow} \text{Dimer})$$

$\Delta G°_{bind}$ is the sum of three terms: ΔE_{intra}, the difference in the internal energy of the two monomers H1 and H2 in the dimer D and the isolated monomers, E_{vdW}, and E_{elec}, the van der Waals and electrostatic inter-helical interactions energies.

$$\Delta G°_{bind} = \Delta E_{intra} + E_{vdW} + E_{elec}$$
$$\Delta E_{intra} = E^{D}_{intra} - E^{H1}_{intra} - E^{H2}_{intra}$$
$$E^{X}_{intra} = E^{X}_{intra,bond} + E^{X}_{intra,vdW} + E^{X}_{intra,elec}$$

Results and discussion

GpA_{TM} dimers

The 1,296 sampled structures formed three families representative of the right-handed, left-handed and parallel dimers with 73, 70 and 16 structures respectively after geometric filters.

Clustering similar structures in each family (Cα RMSD ≤ 2 Å), followed by averaging and MD refinement reduce their population. Finally, four MD models representative of the right-handed helical dimers were obtained, nine are representative of the left-handed dimers and one exhibits parallel helices.

In order to check whether the present protocol allows predicting the experimental structure, Cα RMSDs of all the final MD models relative to two NMR models were calculated. One is the minimized structure of model 16, referred to as $1AFO_{16}$ which exhibits the lowest Cα RMSD value relatively to the 14 final GpA_{TM} MD models. The second is the minimized average NMR structure which will be noted $1AFO_{mean}$. The 20 NMR models are very similar with crossed Cα RMSD values ranging from 0.3 to 1.76 Å. RMSDs of these 20 models from $1AFO_{mean}$ range from 0.34 to 0.94 Å. $1AFO_{16}$ exhibits one of the largest value (0.90 Å). The lowest Cα RMSDs from $1AFO_{16}$ were obtained for the right-handed models ranging from 1.5 to 4.7 Å.

For the left-handed dimers and the parallel dimer RMSDs are greater than 5.9 Å. All the right-handed structures, referred to as GpA_R, show relatively short Cα–Cα distances between the two helices (≤4.4 Å) which are correlated with short distances between the two helical axes (≤7.4 Å).

Table 3 gives the various characteristics of the right-handed models and of two left-handed models, noted here GpA_L, selected on the basis of the strongest helix–helix interactions (GpA_{L1}) and the weakest helix–helix interactions (GpA_{L2}).

Three of the GpA_R models exhibit a crossing angle around –45°, very close to that calculated for $1AFO_{16}$ and $1AFO_{mean}$. Calculated helix–helix angles are also in the range of values derived from MD simulation in membrane (–39° to –46°) (Petrache et al. 2000; Cuthbertson et al. 2006), or in micelles (–44°) (Braun et al. 2004). As shown in Table 3, the magnitude of inter-helical interactions is correlated with the magnitude of accessible SA of the dimer interface. The same is observed for binding free energy. The two left-handed structures exhibit short Cα–Cα residue distances in the same range of value as observed for right-handed dimers. At least, one Gly residue—Gly79 or Gly83—is involved at the dimer interface. Left-handed structures largely differ from the experimental structure $1AFO_{16}$ attested by RMSD values of 5.9 and 6.5 Å. The only parallel dimer resulting from the last filter does not exhibit interesting properties and thus is not discussed here.

It is interesting to remark that the total energy of the different MD dimers around -110 ± 11 kcal mol^{-1} does not allow to differentiate the right-handed and the left-handed structures. The left-handed model GpA_{L1} exhibits the best stability, the strongest helix–helix interactions and, the greatest contacting surface at the interface, but is the furthest from $1AFO_{16}$. The right-handed model GpA_{R1} which is the less stable and shows the weakest helix–helix interactions and the smallest contacting surface is very close to the experimental structure. This is clearly shown by the very low values of RMDS calculated over the residues of the dimerization motif.

Table 3 GpA_{TM} simulated dimer structures

GpA_{TM} models	Ω (°)	D (Å)	$d_{C\alpha-C\alpha}$ (Å)	R_i–R_j	SA (Å^2)	E_{tot} dimer	E_{inter}	$\Delta G°_{bind}$	Cα RMSD (Å)	
									a	b
GpA_{R1}	–44	6.2	4.1	G79–G79	513	–110	–50	–104	1.5*(1.8)*	0.6*(0.7)*
GpA_{R2}	–43	7.0	4.2	G83–M81	585	–118	–57	–132	3.4*(3.3)*	2.9*(2.9)*
GpA_{R3}	–46	6.8	4.0	G86–G86	580	–121	–60	–128	4.7*(4.7)*	4.8*(4.9)*
GpA_{R4}	–35	7.4	4.4	I77–G79	598	–118	–59	–129	3.5*(3.2)*	2.9*(2.8)*
GpA_{L1}	16	8.0	4.5	G79–F78	672	–121	–82	–152	6.5*(6.0)*	4.3*(4.2)*
GpA_{L2}	25	8.9	4.9	G83–V84	528	–100	–43	–79	5.9*(5.4)*	4.0*(3.9)*
$1AFO_{16}$	–50	6.2	3.5	V80–V80	432	–99				
$1AFO_{mean}$	–40	6.9	3.6	V80–V80	424	–100				

The best representative structures of the GpA_{TM} include right-handed coiled-coils (GpA_R) and left-handed coiled-coils (GpA_L). Geometric properties and energy terms are averaged over the last ns of the 4 ns MD simulation. Crossing angle Ω (°) is calculated following a method by Chothia et al. (1981) included in CHARMM. A positive value characterizes a left-handed coiled-coil and a negative value characterizes a right-handed coiled-coil. D (Å): inter-helical distance between the two helices; $d_{C\alpha-C\alpha}$ (Å): minimum distances between Cα atoms of opposed residues; SA (Å^2): contacting surface area at the dimer interface. The two residues in closest proximity are given as R_i–R_j respectively for GpA_{H1} and GpA_{H2}. The total energy of the dimer (E_{tot} dimer) is the sum of the intramolecular energy of the two helices and helix–helix interactions (E_{inter}). $\Delta G°_{bind}$ is the mean value of the binding free energy in the gas-phase (see text for definition). All energy terms are in kcal/mol. Cα RMSD values from the minimized structures $1AFO_{16}$ and $1AFO_{mean}$ (italic) (model 16 and average NMR structure): (a) over all Cα atoms and (b) over the Cα atoms of the GxxxG motif. [RMSD values over the Cα atoms of the seven residues LIxxGVxxGVxxT are very similar (±0.15).] The various geometric and energetic properties are given for the minimized structure

GpA_{TM} dimer interface

Interfacial residues involved in helix–helix association were identified from the Cα–Cα distance maps and the calculations of the buried SAs.

In Fig. 2, the Cα–Cα contact map of GpA_{R1} is compared to that of $1AFO_{16}$ and $1AFO_{mean}$. One may note the strong similarity of distance patterns and particularly that of the two NMR models although model 16 is the more distant from the mean structure. The representation of models clearly confirm their strong similarity.

For GpA_{R1}, the three residues, Gly79, Gly83 and Thr87, have been identified as completely buried. The contact map highlights the well-known interacting residue pairs Gly79–Gly79, Gly83–Gly83, Gly79–Val80 and Gly83–Val80 pertaining to the dimerization motif. In addition to these contacting pairs, others are revealed between Gly83–Val84, Gly79–Ile76, Leu75–Ile76 and the symmetry-related Leu75–Leu75, Ile76–Ile76, and Thr87–Thr87.

For a better comparison with our MD models we have carried on a 4 ns MD simulation of $1AFO_{16}$ and of $1AFO_{mean}$ under the same conditions as described in MD protocol. Mean values of different quantities have been calculated. The Cα–Cα distances less than 6 Å between the two helices are reported in Table 4 for the two experimental models and are compared to those of the six others MD models. It is shown that for both NMR structures, the shortest distances imply the same residues of the GxxxG motif. One may note that the V80–V80 distance evolves from the shortest to the largest during simulation process. We demonstrate that the proximities between the residues of the $G_{79}VMAG_{83}$ motif calculated for GpA_{R1} are almost identical to those of the experimental models. For the others MD models these proximities are not respected.

Our findings are very similar to those obtained recently by (Bu et al. 2007) describing the GpA_{TM} structure using implicit membrane generalized Born model.

The same residue pairs were identified in GpA structures simulated in dimyristoyl-phosphatidylcholine (DMPC) bilayers and dodecyl phosphocholine (DPC) micelles (Cuthbertson et al. 2006).

Although the present study is performed in vacuum the seven residue sequence LIxxGVxxGVxxT is found to be the motif involved in GpA_{TM} helix association.

Surprisingly, even though the close distance between Gly residues at the dimer interface is believed to allow hydrogen bonding interactions between the Thr87 side chains (Cuthbertson et al. 2006) or between the Thr87 side chain and the backbone carbonyl of Val84 residue of the opposed helix (Smith et al. 2002), our simulations did not highlight any Hbond. A possible explanation is that, in micelles, Thr87 can be solvated and water molecules may mediate Hbond interactions between the two side chains (Smith et al. 2002). Also, polar residues are destabilizing residues in detergents and because of helix unravelling Hbonds could be favoured with water (MacKenzie and Engelman 1998). Inter-helical H-bonding interactions are not the only determinant factor for inter-helical association. Other factors can compensate for the loss of this particular interaction.

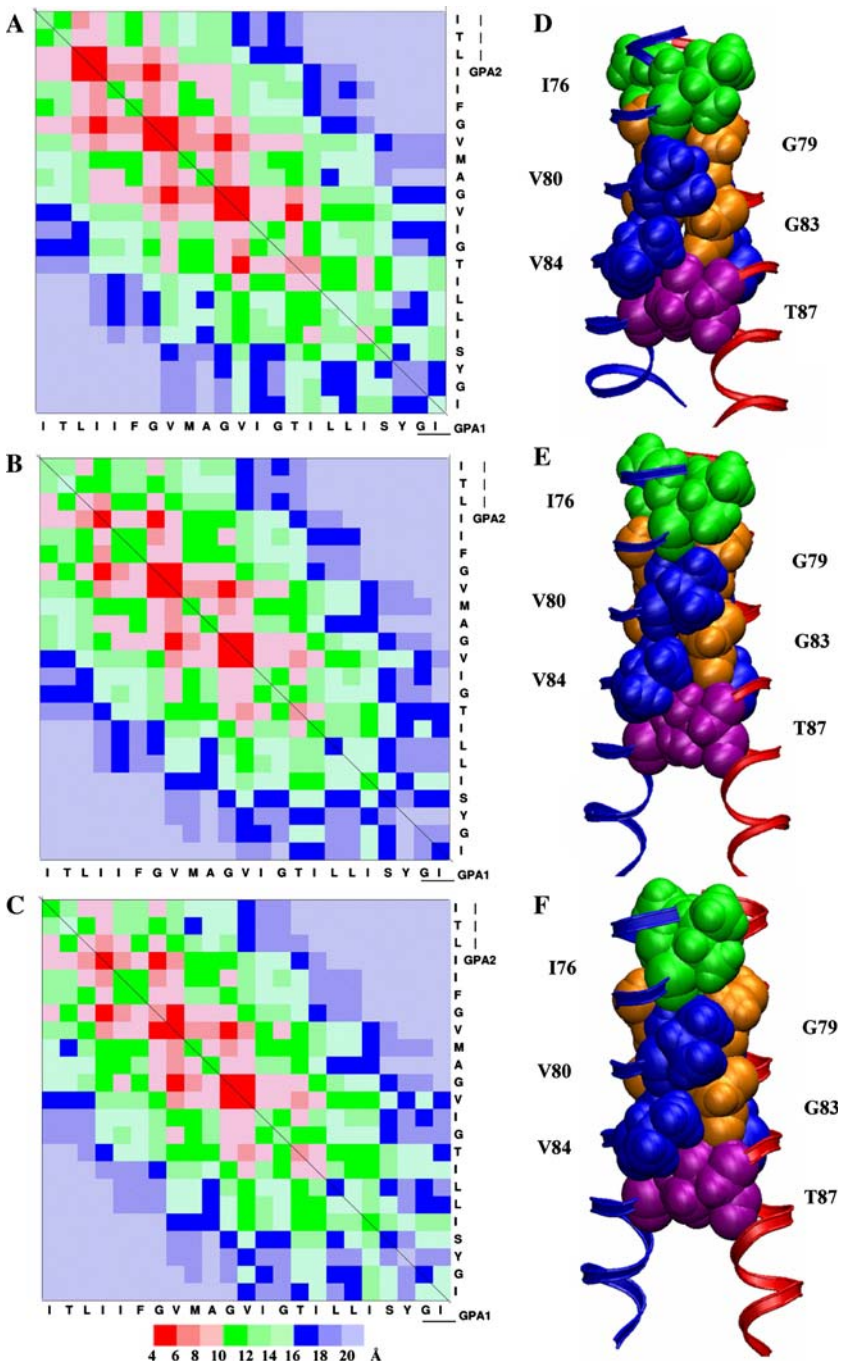

Fig. 2 GpA_{TM} dimer structures. Cα–Cα contact maps of the GpA_{TM} dimer: **a** GpA_{R1} derived from MD search; **b** experimental structure $1AFO_{16}$. (1AFO model 16); **c** average structure of all NMR models. The lowest Cα–Cα distances are in red and the largest distances are in *blue*. The corresponding structures GpA_{R1} (**d**), $1AFO_{16}$ (**e**) and 1AFO average structure (**f**) are shown with the closest residues at the dimer interface

$HER^{2–3}{}_{TM}$ dimers

From the 1,296 sampled structures, three families representative of the right-handed, left-handed and parallel dimers with size of 2, 77 and 20, respectively, were obtained after geometric filters. These first results suggest a strong preference for a left-handed association for the TM domains of the $HER^{2–3}$ heterodimer.

After clustering (Cα RMSD ≤ 2 Å), averaging and MD refinement the number of structures representative of each family is strongly reduced. Only one structure with a right-handed crossing angle was retained and five with a left-handed crossing angle. The dimer with parallel helices resulting from this last step was rejected because of significant distortions at the N-terminal end of both helices. Geometrical properties and energetic data are given in Table 5.

The five left-handed structures are slightly different or relatively different as attested by the Cα RMSD values that compare all the structures (between 2.7 and 5.1 Å). The

Table 4 Cα–Cα distances (≤ 6 Å) calculated between the residues of the two helices R_i–R_j for the MD models predicted for GpA_{TM} dimer (right-handed and left-handed) and for the two NMR structures: $1AFO_{16}$ (model 16) and the average structure of the 20 NMR models ($1AFO_{mean}$)

R_i–R_j	GpA_{R1}	GpA_{R2}	GpA_{R3}	GpA_{R4}	GpA_{L1}	GpA_{L2}	$1AFO_{mean}$		$1AFO_{16}$	
G79–G79	4.14						4.31	*4.48*	4.26	*5.11*
G83–V80	4.28						4.29	*4.58*	4.78	*4.31*
G83–G83	4.40						4.43	*5.35*	4.40	*5.19*
V80–G79	4.50			5.03			4.53	*4.49*	4.80	*4.29*
V80–G83	4.56						4.66	*4.66*	4.22	*4.17*
G79–V80	4.64	5.00					4.88	*4.88*	4.50	*4.23*
V80–V80	5.19						5.24	*5.24*	5.27	*3.51*
G83–M81		4.16			4.79					
G79–M81		4.61			5.33	5.31				
A82–M81		5.86								
V80–M81		5.86				5.60				
A82–A82			4.61							
M81–G79				4.51						
M81–G83				4.58						
M81–V80				5.76						

Values are averaged over the last ns of the simulation. Values from the minimized structures are in italic

crossing angle ranges from 13° and 31°. As shown in Table 5, all these models exhibit energetically stable structural arrangement of the helices leading to stable dimers. Inter-helical interactions differ at the most by 20 kcal/mol and difference in internal energy of the dimers between the lowest structure and the weakest structure is in the same range of value. Energetic factors are not sufficient to distinguish the most representative structure of the TM domain of the HER^{2-3} heterodimer. The structure of this domain is unknown and any structural data is available. The only information which can be used to select the best representative structure of the $HER^{2-3}{}_{TM}$ domain is the presence of the GxxxG-like motif at the dimer interface. As revealed by numerous studies on TM helices of membrane proteins this motif is presumed to drive helix–helix association (Russ and Engelman 2000; Dawson et al. 2002; Mendrola et al. 2002; Arselin and Giraud 2003; McClain et al. 2003). This hypothesis is confirmed by biological studies on HER_{TM} domains (Mendrola et al. 2002; Gerber et al. 2004). Three dimer models conform to this hypothesis with similar free binding energy values. One is the right-handed structure referred to as $HER^{2-3}{}_{R}$, the two others are the left-handed structures refereed to as $HER^{2-3}{}_{L1}$ and $HER^{2-3}{}_{L2}$. Helix–helix interface of these three structures are detailed below.

$HER^{2-3}{}_{TM}$ dimer interface

The Cα–Cα distance maps and the views of $HER^{2-3}{}_{R}$, $HER^{2-3}{}_{L1}$ and $HER^{2-3}{}_{L2}$ structures are shown in Fig. 3. The contact map relative to the right-handed structure (a) shows that the shortest distances involve the N-terminal

Table 5 $HER^{2-3}{}_{TM}$ simulated dimer structures

$HER^{TM}{}_{2-3}$ models	Ω (°)	*D* (Å)	$d_{Cα–Cα}$ (Å)	R_i–R_j	SA (Å^2)	E_{tot} dimer	E_{inter}	$\Delta G°_{bind}$
$HER_R{}^{2-3}$	–20	8.3	5.6	L663–I665	716	–162	–59	–157
$HER_{L1}{}^{2-3}$	24	8.1	4.4	A657–T647	687	–175	–65	–161
$HER_{L2}{}^{2-3}$	31	7.8	5.5	S656–V648	694	–167	–53	–152
$HER_{L3}{}^{2-3}$	22	8.5	5.2	I673–L659	636	–154	–53	–140
$HER_{L4}{}^{2-3}$	13	8.7	4.8	G668–G660	590	–168	–42	–140
$HER_{L5}{}^{2-3}$	26	8.0	5.1	S656–T647	693	–173	–63	–169

The best representative structures of the $HER^{2-3}{}_{TM}$ include right-handed coiled-coils ($HER^{2-3}{}_{R}$) and left-handed coiled-coils ($HER^{2-3}{}_{L}$). Geometric properties and energy terms are averaged over the last ns of the 4 ns MD simulation. Definitions of the geometric parameters, crossing angle Ω (°), *D* (Å), $d_{Cα–Cα}$ (Å), SA (Å^2) and energy terms (in kcal/mol) are defined as in Table 3. The two residues in closest proximity are given as R_i–R_j respectively for $HER^2{}_{TM}$ and $HER^3{}_{TM}$

residues of the helices. The shortest proximities are observed for the following residue pairs: L651T652–T643M644, T652–T647, V655S656–T647V648, V655–M644, S656–G651, V659–V648, V659–G651L652, L663–I655 and L667–L659. Contacting maps of the two left-handed structures are slightly different. The closest proximities are observed between the N-terminal residues for $HER^{2–3}{}_{L1}$ (b) while they are observed all along the TM sequences for $HER^{2–3}{}_{L2}$ (c). In the case of $HER^{2–3}{}_{L1}$, the shortest distances involve the following residue pairs S656–T647, A657–T647, G660–A650, G660–G651, I661–A650 at the N-terminus and F671–G661 at the C-terminus. For $HER^{2–3}{}_{L2}$, a strong implication of S656 and G660 of the $HER^{2}{}_{TM}$ and T647 and G651 of $HER^{3}{}_{TM}$ are revealed. One may remark a strong implication of the C-terminal residues and particularly those of the C-terminal GxxxG-like motif of $HER^{2}{}_{TM}$. All the three structures clearly exhibit the N-terminal GxxxG-like motif at the dimer interface. All the residues involved in short interfacial Cα–Cα distances are completely or almost completely buried.

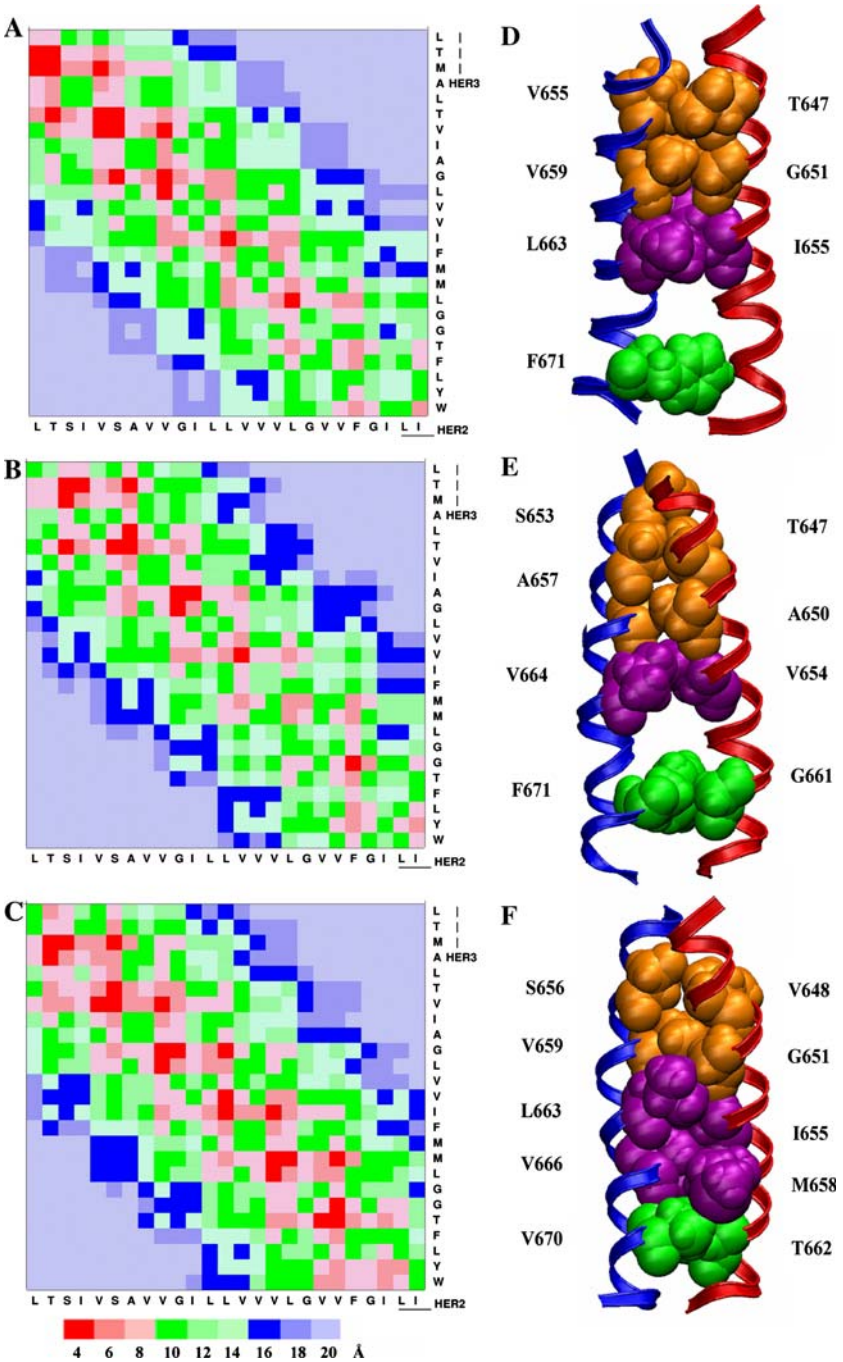

Fig. 3 $HER^{2–3}{}_{TM}$ dimer structures. Cα–Cα contact maps of the representative models of $HER^{2–3}{}_{TM}$ dimer derived from MD search: right-handed structure $HER^{2–3}{}_{R1}$ (**a**), left-handed structures $HER^{2–3}{}_{L1}$ (**b**) and $HER^{2–3}{}_{L2}$. (**c**). The lowest Cα–Cα distances are in *red* and the largest distances are in *blue*. The corresponding structures $HER^{2–3}{}_{R1}$ (**d**), $HER^{2–3}{}_{L1}$ (**e**) and $HER^{2–3}{}_{L2}$ (**f**) are shown with the closest residues at the dimer interface. Backbone ribbon of $HER^{2}{}_{TM}$ helix is in *blue* and that of $HER^{3}{}_{TM}$ helix is in *red*. At the N-terminus, buried residues of the GxxxG-like motif are colored *orange*, buried residues at the C-terminus including residues of the GxxxG-like motif of $HER^{2}{}_{TM}$ are shown in *green*. Other buried residues are in *purple*

Concluding discussion

In the present study, we show that sequence information and oligomerization state are sufficient to predict structural models of TM helix assembly.

Because MD simulations in membrane are very time consuming, our study, as most of others that aimed to explore the conformational space of helix–helix assembly are undertaken in vacuum (Adams et al. 1995; Torres et al. 2001; Caballero-Herrera and Nilsson 2003). It is largely admitted that helix–helix contacts are the main factor that govern helix–helix association and that the membrane environment does not exert major effects (White and Wimley 1999). Membrane acts as a modulator of the stability of oligomers (Petrache et al. 2000; Cuthbertson et al. 2006). The conformational space explored in vacuum is very close to that explored in hydrated lipids (Duneau et al. 1999a, b). Thus one may think that the structures predicted in vacuum are close to those in a real membrane provided that they respect the properties of the membrane/solvent environment.

Our approach is based on the global searching method developed for predicting HER2/Neu homodimers (Garnier et al. 1997; Sajot and Genest 2000) and was revisited to explore the whole conformational space without imposing limitation. This is in contrast to several other methods that impose rotational symmetry, helix tilt angle or helix–helix angle (Krogh et al. 2001; Chen et al. 2002; Kim et al. 2003; Kokubo and Okamoto 2004; Akula and Pattabiraman 2005; Adamian and Liang 2006; Beevers and Kukol 2006; Fleishman et al. 2006b; Bu et al. 2007). Another advantage is the MD exploration of a relatively limited number of configurations for a given heterodimer system. Thus, the present approach is very attractive to define rapidly, without a priori, an ensemble of structures representative of the native state of TM heterodimers. Such an approach could be broaden to the prediction of larger oligomeric states by taking into account additional criteria as those deduced from statistical analysis of membrane proteins.

The present MD search protocol is successful in predicting the structure of the GpA_{TM} dimer. Any quantitative experimental data is used except the knowledge of the proximity of the GxxxG motifs at the dimer interface.

Obviously, the success of a prediction method is difficult to evaluate without experimental data. In the present work, only geometric criteria are used to propose reasonable structures of two interacting helices. One difficulty is to define a suitable balance between the number of filters and their degree of severity to minimize the risk to predict wrong structures. More the number of filters is large, less is the risk. More accurate prediction imposes the use of experimental data, at least qualitative.

The question of the correctness of a predictive method for describing the structure of helix–helix assembly is of major importance owing to the difficulty of experimental studies in membrane environment. The biological importance of the HER receptors and the lack of knowledge of homo and hetero dimerization processes lead us to investigate structural models of the TM domain. Structural models of the $HER^{2-3}{}_{TM}$ domain are proposed, based only on the presence of the GxxxG-like dimerization motif at helix–helix interface (Mendrola et al. 2002). As discussed above, one may think that they are representative of the structures in the membrane environment.

The present method is currently used for the prediction of the structures of the TM domain of all HER heterodimers with the aim to give insights into the hierarchical network of inter receptor interactions that determine signal transduction (Tzahar et al. 1996; Duneau et al. 2007).

References

Adamian L, Liang J (2006) Prediction of transmembrane helix orientation in polytopic membrane proteins. BMC Struct Biol 6(1):13

Adams PD, Arkin IT et al (1995) Computational searching and mutagenesis suggest a structure for the pentameric transmembrane domain of phospholamban. Nat Struct Biol 2(2):154–162

Adams PD, Engelman DM et al (1996) Improved prediction for the structure of the dimeric transmembrane domain of glycophorin A obtained through global searching [published erratum appears in Proteins 1997 Jan;27(1):132]. Proteins 26:257–261

Akula N, Pattabiraman N (2005) A systematic search method for the identification of tightly packed transmembrane parallel alpha-helices. J Biomol Struct Dyn 22(6):625–634

Arselin G, Giraud MF (2003) The GxxxG motif of the transmembrane domain of subunit e is involved in the dimerization/oligomerization of the yeast ATP synthase complex in the mitochondrial membrane. Eur J Biochem 270(8):1875–1884

Beevers AJ, Kukol A (2006) Systematic molecular dynamics searching in a lipid bilayer: application to the glycophorin A and oncogenic ErbB-2 transmembrane domains. J Mol Graph Model 25:226–233

Berman HM, Battistuz T et al (2002) The Protein Data Bank. Acta Crystallogr D Biol Crystallogr 58(Pt 6 No 1):899–907

Beuming T, Weinstein H (2005) Modeling membrane proteins based on low-resolution electron microscopy maps: a template for the TM domains of the oxalate transporter OxlT. Protein Eng Des Sel 18(3):119–125

Bowie JU (1997) Helix packing in membrane proteins. J Mol Biol 272:780–789

Braun R, Engelman DM et al (2004) Molecular dynamics simulations of micelle formation around dimeric glycophorin A transmembrane helices. Biophys J 87(2):754–763

Brooks BR, Bruccoleri RE, Olafson BD, States DJ, Swaminathan S, Karplus M (1983) CHARMM: a program for macromolecular energy minimization, and dynamics calculations. J Comp Chem 4:187–217

Bu L, Im W et al (2007) Membrane assembly of simple helix homo-oligomers studied via molecular dynamics simulations. Biophys J 92(3):854–863

Bywater RP, Thomas D et al (2001) A sequence and structural study of transmembrane helices. J Comput Aided Mol Des 15(6):533–552

Caballero-Herrera A, Nilsson L (2003) Molecular dynamics simulations of the E1/E2 transmembrane domain of the Semliki Forest virus. Biophys J 85(6):3646–3658
Chen CP, Kernytsky A et al (2002) Transmembrane helix predictions revisited. Protein Sci 11(12):2774–2791
Chothia C, Levitt M et al (1981) Helix to helix packing in proteins. J Mol Biol 145:215–250
Citri A, Skaria KB et al (2003) The deaf and the dumb: the biology of ErbB-2 and ErbB-3. Exp Cell Res 284(1):54–65
Coussens L, Yang-Feng TL et al (1985) Tyrosine kinase receptor with extensive homology to EGF receptor shares chromosomal location with neu oncogene. Science 230(4730):1132–1139
Cuthbertson JM, Bond PJ et al (2006) Transmembrane helix–helix interactions: comparative simulations of the glycophorin a dimer. Biochemistry 45(48):14298–14310
Dawson JP, Weinger JS et al (2002) Motifs of serine and threonine can drive association of transmembrane helices. J Mol Biol 316(3):799–805
Duneau JP, Crouzy S, Chapron Y, Genest M (1999a) Dynamics of the transmembrane domain of the ErbB-2 receptor. Theor Chem Acc 101(1–3):87–91
Duneau JP, Crouzy S et al (1999b) Molecular dynamics simulations of the ErbB-2 transmembrane domain within an explicit membrane environment: comparison with vacuum simulations. Biophys Chem 76(1):35–53
Duneau JP, Vegh AP et al (2007) A dimerization hierarchy in the transmembrane domains of the HER receptor family. Biochemistry 46(7):2010–2019
Ehsani A, Low J et al (1993) Characterization of a new allele of the human ERBB2 gene by allele-specific competition hybridization. Genomics 15(2):426–429
Eilers M, Shekar SC et al (2000) Internal packing of helical membrane proteins. Proc Natl Acad Sci USA 97(11):5796–5801
Fleishman SJ, Schlessinger J et al (2002) A putative molecular-activation switch in the transmembrane domain of erbB2. Proc Natl Acad Sci USA 99(25):15937–15940
Fleishman SJ, Harrington S et al (2004) An automatic method for predicting transmembrane protein structures using cryo-EM and evolutionary data. Biophys J 87(5):3448–3459
Fleishman SJ, Ben-Tal N (2006a) Progress in structure prediction of alpha-helical membrane proteins. Curr Opin Struct Biol 16(4):496–504
Fleishman SJ, Unger VM et al (2006b) Transmembrane protein structures without X-rays. Trends Biochem Sci 31(2):106–113
Garnier N, Genest D et al (1997) Molecular modeling of c-erbB2 receptor dimerization: coiled-coil structure of wild and oncogenic transmembrane domains. Stabilization by interhelical hydrogen bonds in the oncogenic form. Biopolymers 42(2):157–168
Gerber D, Sal-Man N et al (2004) Two motifs within a transmembrane domain, one for homodimerization and the other for heterodimerization. J Biol Chem 279(20):21177–21182
Gimpelev M, Forrest LR et al (2004) Helical packing patterns in membrane and soluble proteins. Biophys J 87(6):4075–4086
Graus-Porta D, Beerli RR et al (1997) ErbB-2, the preferred heterodimerization partner of all ErbB receptors, is a mediator of lateral signaling. Embo J 16(7):1647–1655
Herzyk P, Hubbard RE (1995) Automated method for modeling seven-helix transmembrane receptors from experimental data. Biophys J 69(6):2419–2442
Jayasinghe S, Hristova K et al (2001) Energetics, stability, and prediction of transmembrane helices. J Mol Biol 312(5):927–934
Kallblad P, Dean PM (2004) Backbone-backbone geometry of tertiary contacts between alpha-helices. Proteins 56(4):693–703
Killian JA (2003) Synthetic peptides as models for intrinsic membrane proteins. FEBS Lett 555(1):134–138
Killian JA, von Heijne G (2000) How proteins adapt to a membrane-water interface. T.I.B.S. Trends Biochem Sci 25:429–434
Kim S, Chamberlain AK et al (2003) A simple method for modeling transmembrane helix oligomers. J Mol Biol 329(4):831–840
Kokubo H, Okamoto Y (2004) Prediction of membrane protein structures by replica-exchange Monte Carlo simulations: case of two helices. J Chem Phys 120(22):10837–10847
Kraus MH, Issing W et al (1989) Isolation and characterization of ERBB3, a third member of the ERBB/epidermal growth factor receptor family: evidence for overexpression in a subset of human mammary tumors. Proc Natl Acad Sci USA 86(23):9193–9197
Krogh A, Larsson B et al (2001) Predicting transmembrane protein topology with a hidden Markov model: application to complete genomes. J Mol Biol 305(3):567–580
MacKenzie KR, Engelman DM (1998) Structure-based prediction of the stability of transmembrane helix–helix interactions: the sequence dependence of glycophorin A dimerization. Proc Natl Acad Sci USA 95(7):3583–3590
MacKenzie KR, Prestegard JH et al (1997) A transmembrane helix dimer: structure and implications. Science 276:131–133
MacKerell JAD, Bashford D, Bellot M, Dunbrack RL, Evansek JD, Field MJ, Fisher S, Gao J, Guo H, Ha S, Joseph McCarthy D, Kuchnir L, Kuczera K, Lau FTK, Mattos C, Michnick S, Ngo T, Nguyen DT, Prodohm B, Reiher WE, Roux B, Schlenkrich B, Smith J, Stote R, Straub J, Watanabe M, Wiorkiewicz-Kuczera J, Karplus M (1992) Self-consistent parametrization of biomolecules for molecular modelling and condensed phase simulations. Biophys J 61:A143
McClain MS, Iwamoto H et al (2003) Essential role of a GXXXG motif for membrane channel formation by Helicobacter pylori vacuolating toxin. J Biol Chem 278(14):12101–12108
Mendrola JM, Berger MB et al (2002) The single transmembrane domains of ErbB receptors self-associate in cell membranes. J Biol Chem 277(7):4704–4712
Opella SJ, Marassi FM (2004) Structure determination of membrane proteins by NMR spectroscopy. Chem Rev 104(8):3587–3606
Petrache HI, Grossfield A et al (2000) Modulation of Glycophorin A transmembrane helix interactions by lipid bilayers: molecular dynamics calculations. J Mol Biol 302:727–746
Pinkas-Kramarski R, Soussan L et al (1996) Diversification of Neu differentiation factor and epidermal growth factor signaling by combinatorial receptor interactions. EMBO J 15:2452–2467
Popot JL, Engelman DM (1990) Membrane protein folding and oligomerization: the two-stage model. Biochemistry 29:4031–4037
Rubin I, Yarden Y (2001) The basic biology of HER2. Ann Oncol 12(Suppl 1):S3–S8
Russ WP, Engelman DM (2000) The GxxxG motif: a framework for transmembrane helix–helix association. J Mol Biol 296(3):911–919
Ryckaert JP, Ciccotti G et al (1977) Numerical integration of cartesian equations of motion of a system with constraints: molecular dynamics of *n*-alkanes. J Comput Phys 23:327
Sajot N, Genest M (2000) Structure prediction of the dimeric neu/ErbB-2 transmembrane domain from multi-nanosecond molecular dynamics simulations. Eur Biophys J 28(8):648–662
Schlessinger J (2000) Cell signaling by receptor tyrosine kinases. Cell 103(2):211–225
Senes A, Engel DE et al (2004) Folding of helical membrane proteins: the role of polar, GxxxG-like and proline motifs. Curr Opin Struct Biol 14(4):465–479
Smith SO, Eilers M et al (2002) Implications of threonine hydrogen bonding in the glycophorin A transmembrane helix dimer. Biophys J 82(5):2476–2486
Tanner KG, Kyte J (1999) Dimerization of the extracellular domain of the receptor for epidermal growth factor containing the mem-

brane-spanning segment in response to treatment with epidermal growth factor. J Biol Chem 274(50):35985–35990

Tomita M, Furthmayr H et al (1978) Primary structure of human erythrocyte glycophorin A. Isolation and characterization of peptides and complete amino acid sequence. Biochemistry 17(22):4756–4770

Torres J, Kukol A et al (2001) Mapping the energy surface of transmembrane helix–helix interactions. Biophys J 81(5): 2681–2692

Treutlein HR, Lemmon MA et al (1992) The glycophorin A transmembrane domain dimer: sequence-specific propensity for a right-handed supercoil of helices. Biochemistry 31:12726–12733

Tzahar E, Waterman H et al (1996) A hierarchical network of interreceptor interactions determines signal transduction by Neu differentiation factor/neuregulin and epidermal growth factor. Mol Cell Biol 16(10):5276–5287

White SH (2004) The progress of membrane protein structure determination. Protein Sci 13(7):1948–1949

White SH, Wimley WC (1999) Membrane protein folding and stability: physical principles. Annu Rev Biophys Biomol Struct 28:319–365

White SH, Ladokhin AS et al (2001) How membranes shape protein structure. J Biol Chem 276(35):32395–32398

Yamamoto T, Ikawa S et al (1986) Similarity of protein encoded by the human c-erb-B-2 gene to epidermal growth factor receptor. Nature 319:230–234

Zoete V, Meuwly M et al (2005) Study of the insulin dimerization: binding free energy calculations and per-residue free energy decomposition. Proteins 61(1):79–93